Environ. Sci. Technol. **1998**, *32,* 1841−1846

Selenium Removal Using Ca-Based Sorbents: Reaction Kinetics

R. AGNIHOTRI, S. CHAUK, S. MAHULI, AND L.-S. FAN*

Department of Chemical Engineering, The Ohio State University, Columbus, Ohio 43210

Selenium, along with mercury and halides, represents one of the most volatile trace metallic emissions from coal-fired combustors and utility boilers. Calcium-based sorbents are shown to capture selenium oxide via a chemical reaction leading to the formation of calcium selenite. In this study, intrinsic kinetics of this chemical interaction is investigated. Experiments are conducted to obtain initial reaction rate and to determine basic kinetic parameters such as activation energy of the reaction, order of reaction with respect to the gas-phase selenium concentration, and influence of sorbent initial surface area. Experimental investigations are conducted in a differential-bed flow-through reactor system at 400−600 °C temperature conditions with SeO_2 partial pressure in the range of 5−30 Pa. Activation energy of the reaction of 4.03 kcal/gmol is obtained, and the reaction is found to have an order of 0.67, with respect to SeO_2 partial pressure. Rate of reaction is determined to vary with the initial sorbent surface area. Sorption of selenium oxide in the presence of SO_2 in the gas phase suggests that the two reactions are competitive, and the formation of $CaSeO_3$ is considerably slower than the sulfation of the sorbent when the concentration of the two species in the gas phase is comparable. This suggests that the reaction between sorbent particles and SeO_2 is insignificant in the presence of SO_2.

Introduction

It is well documented that coal combustion, waste incineration, metallurgical processes, and glass manufacturing generate gaseous effluents containing selenium or its oxide species (*1*−*4*). Selenium is one of the most volatile trace elements, second only to mercury and halide species, in coal, and a significant portion of it escapes to the atmosphere in vapor form (*4*, *5*). A number of prior investigations (*4*−*7*) have shown that a substantial amount of selenium in the exiting flue gas from coal-fired combustors and utility boilers remains in gas phase. It is distributed between the vapor and condensed forms depending upon various factors such as initial concentration in the parent coal, design and operating conditions of the combustion facility, and particulate control devices. Germani and Zoeller (*5*) reported an average of 59% of the in-stack Se to be in the form of vapor and its concentration in the vapor phase to be about 25 $\mu g/m^3$. Mercury and the halogens are the only other elements that exhibit such high affinity for the gas phase. Selenium and its compounds have been linked to harmful toxicological impacts despite the fact that Se is an essential trace element for humans and other animals (*8*−*10*). Coal-fired power plants have been identified as major sources responsible for trace metal emissions including selenium and will most likely be required to reduce these emissions by impending EPA regulations.

Title III of the Clean Air Act Amendment of 1990 identifies a host of hazardous air pollutants (HAPs) as sources of potential air pollution with impending regulations. Most of these 189 HAPs are emitted in trace amounts from coal-fired combustors and utility boilers. In case of selenium, the inclusion of coal-burning facilities is highly probable since, in an estimate, 62% of industrial selenium emission has been linked to these sources (*11*). Average selenium content of U.S. coal is reported as 4 ppm (*12*).

Selenium is similar to sulfur in most of its chemistry, and −2, 0, +2, +4, and +6 are its possible oxidation states. Thus under changing conditions of temperature and diverse chemical composition, selenium can exist in flue gas in various chemical forms. However, not all the forms of selenium are thermodynamically stable, and it is suggested that selenium in flue gas predominantly exists in elemental state (Se) and/or the oxide form (SeO_2, oxidation state +4) depending upon the temperature and flue gas composition. Andren et al. (*4*) utilized a series of chemical tests to conclude that nearly all the Se in the flue gas exists as elemental Se. They postulated that at low temperatures (less than 150 °C) the SO_2 produced during coal combustion could act as a reducing agent to yield elemental Se from SeO_2. Davison et al. (*13*) concluded from the thermodynamic data that it is SeO_2 that escapes to the atmosphere and at 25 °C as much as 80 $\mu g/m^3$ Se can exist as SeO_2. Oehm et al. (*10*) suggested the reaction of SeO_2 with moisture could lead to the formation of selenous acid (H_2SeO_3) in atmospheric aerosols. Later studies (*14*) indicate that selenium exists as SeO_2 for almost the entire course of its stay in the combustion environment, but at the lower temperatures of the stack, it could be partially reduced to Se by the presence of SO_2.

The high volatility and its existence in the form of vapor make selenium emission control a very difficult task. A reduction in the operating temperature of the stack could enhance condensation of the vapor and hence metal removal, but the resulting loss in buoyancy of the stack emission eliminates this as a feasible technique. Improving performance of the particulate control device can lead to better capture of the finer metal aerosols; however, it fails to lessen the gas-phase emission. In the past few years, dry sorbent injection for in-situ capture of the metal from hot flue gas has been studied with the aim of developing a potential control technique. The rationale behind such an approach lies in its already proven performance in SO_2 removal by using calcium-based sorbents in high or medium temperature range of the flue gas pathway. In dry sorbent injection technique, metal sorption by the solid could take place by means of physical adsorption, chemisorption, chemical reaction, or a combination of these processes. Prior investigations (*15*−*19*) have involved studies on the effectiveness of different mineral sorbents in the removal of cadmium, lead, and alkali metal compounds from hot flue gas. The effectiveness of calcium-based sorbents, especially hydrated lime ($Ca(OH)_2$), has been demonstrated for the removal of selenium (*18, 19*). The results of studies by Ghosh-Dastidar et al. (*19*) have shown that the mechanism of capture by $Ca(OH)_2$ is not a simple physical adsorption process but involves a chemical reaction between CaO and SeO_2. They found the medium temperature range of 400−600 °C to be most favorable for the reaction to occur and leads to high

* To whom correspondence should be addressed. Telephone: (614)292-7907; fax: (614)292-3769; e-mail: Fan@kcgl1.eng.ohio-state.edu.

S0013-936X(97)01119-X CCC: $15.00
Published on Web 04/29/1998

selenium sorption. At higher temperatures, thermodynamic equilibrium aids dissociation of the reaction product, and the amount of metal capture reduces drastically with increasing temperature. They confirmed the formation of calcium selenite as the reaction product by conducting extensive postsorption analyses of the sorbent using X-ray diffraction, ion chromatography, and various other spectroscopic techniques. The following reaction scheme has been proposed by these researchers for Se capture using $Ca(OH)_2$:

$$Ca(OH)_2 = CaO + H_2O \quad (1a)$$

$$CaO + SeO_2 = CaSeO_3 \quad (1b)$$

In recent years, research has been focused toward finding multi-functional sorbents that are suitable for removing a number of air toxins. Calcium-based sorbents have been used extensively for the removal of acidic gases, and they offer an attractive option for use as multifunction sorbents because of their performance in capturing sulfur and selenium species. Sulfation kinetics of these sorbents have been extensively studied, but studies addressing the interaction of SeO_2 with Ca-based sorbents under typical flue gas environment are lacking. In the actual flue gas atmosphere, Ca-based sorbents can react with a host of constituents, and the extent to which one particular species is captured depends greatly on the kinetics of the reaction between that species and the sorbent. It is very well documented that the sulfation reaction of Ca sorbents is rapid (*20, 21*). To realize the role of Ca-based sorbents as multi-functional sorbents and to determine the effectiveness of these sorbents in removing Se species from flue gas, it is imperative that SeO_2 interaction kinetics of these sorbents be investigated. Furthermore, studies must be undertaken to investigate simultaneous removal of SO_2 and SeO_2 from hot flue gas environment to fully realize the multi-functional role of Ca-based sorbent.

In this study, the kinetics of reaction between selenium oxide and CaO are investigated. Experiments are conducted to determine the basic kinetic parameters such as activation energy of the reaction, order of reaction with respect to the gas-phase selenium concentration, and influence of initial sorbent structural properties. Experimental investigations are also undertaken to study the simultaneous removal of SO_2 and SeO_2 in this study.

Experimental Section

The schematic of the differential reactor assembly is shown in Figure 1. The main components of this system are the microbalance-equipped toxic vapor generation assembly that is interfaced with a PC-based data acquisition assembly, a high-temperature three-way valve, and the differential bed assembly housed in a furnace. The details of the reactor system are described elsewhere (*19, 22*).

Vapor Generation Assembly. The selenium source is held in a Pt sample pan suspended by a Pt hangdown wire from the ATI Cahn D-200 digital microbalance. As suggested in the literature (*14*), in the temperature range of interest SeO_2 is the most thermodynamically favored form, and thus SeO_2 is used as the selenium source in all the experiments. The vaporization tube that houses the source pan is a 25.4 mm o.d. quartz tube with provision for carrier gas entry and thermocouple insertion for monitoring the source temperature. Dry nitrogen, which is used as the carrier gas in all the experiments, enters at the top of the tube and flows down over the selenium source. The vaporization tube is wrapped with heating tape and closely maintained at a specific temperature using the thermocouple and a temperature controller. Solid SeO_2 sublimes at a temperature of 317 °C. The desired concentration of selenium in the gas phase

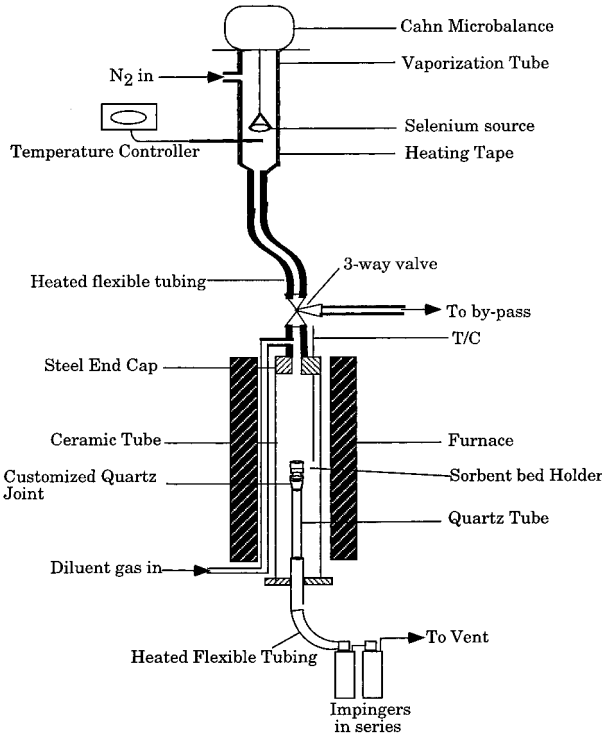

FIGURE 1. Schematic of differential bed reactor (DBR) system.

dictates the temperature at which the vaporization tube is maintained. The flow rate of the carrier gas is maintained at 0.50 L/min (STP). The rate of selenium dioxide vaporization is critical toward maintaining a constant SeO_2 gas phase concentration. Experiments are conducted under a constant SeO_2 vaporization rate, ensuring near-constant SeO_2 concentration in the reactor. During the period of unsteady vaporization rate, SeO_2 vapors are not sent into the reactor and are bypassed to the scrubbers.

Reactor Assembly. The reactor assembly consists of a ceramic tube, a 1200 °C Lindberg single-zone furnace, and a sorbent holder assembly. The reactor is a 25.4 mm o.d. mullite tube cemented to custom-fabricated stainless steel end-connections at the top and bottom. The top connection has provision for mixing the toxic vapor-laden reactant stream with the diluent flow. A 6.4 mm o.d. flexible stainless steel tubing transports the SeO_2-carrying gas from the vaporization tube to the top of the reactor. Selenium vapors generated in the vaporization tube can either be introduced into the reactor or can be sent to the bypass scrubber via a high-temperature three-way valve. To avoid condensation in the bypass line and valve, the temperature of the valve assembly is constantly maintained at 10 °C higher than the vaporization temperature. Addition of a three-way valve helps in conducting short-contact time sorption experiments. Before the carrier gas enters the reactor, it is mixed with diluent gas. Dry nitrogen is used as the diluent stream. This serves to adjust the concentration of the Se species in the reactor to the desired levels. For all the experiments, diluent gas flow is maintained at 2.0 L/min (STP). The diluent gas stream is preheated to the reactor temperature prior to entering the reactor and mixing with the carrier gas. Mixing of the diluent gas and the carrier gas takes place at the top of the reactor. The sorbent is dispersed on a small amount of quartz wool that is supported on the quartz sorbent holder of 10.0 mm o.d. and is cemented to a 12.7 mm o.d. stainless steel tube through which all the reactant gases (2.5 L/min at STP) are transported out after flowing through the sorbent bed. The superficial gas velocity through the sorbent holder is maintained at 0.4 m/s to ensure that external mass transfer

resistance is negligible. The sorbent holder assembly is inserted inside the reactor from the bottom and is positioned such that the bed lies near the center of the furnace heating section. The gas coming out from the reactor passes through a train of scrubbers to capture the remaining SeO_2 before being vented to exhaust. A 7% by weight HNO_3 solution is used as the scrubber solution.

Sorbent−SeO_2 interaction is studied in the temperature range of 400−600 °C. At temperatures above 700 °C (*23*), the decomposition of $CaSeO_3$ becomes significant, and at temperatures below 300 °C, physical adsorption of SeO_2 on the sorbent could interfere with reaction kinetics. This is corroborated by earlier researchers (*19*), who have also observed that the optimum temperature range for SeO_2 capture by CaO is the medium temperature range of 400−600 °C.

Three different CaO sorbents of varying surface areas are used to study the effect of surface area on reaction kinetics. The highest surface area (52 m^2/g) was obtained from calcination of $Ca(OH)_2$ at 800 °C for 10 min under nitrogen flow followed by exposure to SeO_2. CaO of surface area 35 m^2/g is also prepared in a similar manner by calcination of $Ca(OH)_2$ at a temperature 1000 °C for 10 min. CaO of least surface area is purchased from Mississippi Lime Company and is stored under nitrogen to avoid rehydration and recarbonation.

Postsorption Sorbent Analyses: Product Identification. Sorbent samples following adsorption are analyzed using a battery of analytical techniques such as X-ray diffraction (XRD), ion chromatography (IC), X-ray photoelectron spectroscopy (XPS), and atomic absorption spectroscopy (AAS). The amount of selenium captured is determined using AAS, and the chemical form of the captured selenium is identified using XRD, IC, and XPS. A detailed description of the procedures for obtaining direct experimental evidence supporting the proposed reaction and stoichiometry are given elsewhere (*19*).

Kinetic Model Development

To determine the basic kinetic parameters of a gas−solid reaction, it is essential to perform experiments with minimal transport resistance. The rate of gas−solid reactions is governed by a combination of resistances associated with reaction, external mass transfer between the bulk gas phase and solid surface, product layer diffusion, and internal diffusion. External mass transfer resistance is dominating at the initial stages of the reactions and can be made negligible if the gas flow rate is kept sufficiently high and the system is a flow-through system as opposed to a flow-over system as is the case in studies conducted in a thermal gravimetry-based reactor systems. Product layer diffusion becomes critical with increasing conversion and product layer thickness. This resistance can be neglected for very small conversions as is the case in initial rate studies. Under appropriate conditions, initial reaction rate data can be applied to calculate the activation energy and order of reaction. The reaction between SeO_2(g) and CaO(s) is represented by

$$SeO_2(g) + CaO(s) = CaSeO_3(s) \tag{2}$$

In the initial stages, the reaction rate can be given by the following general reaction rate equation

$$-r_{init} = \left(\frac{dx}{dt}\right)_{init} = k{P_{SeO_2}}^m {A_{CaO}}^n \tag{3}$$

and

$$A_{CaO} = S_o(1 - x) \tag{4}$$

where k is the rate constant of the reaction; n and m are the orders of reaction with respect to solid and gaseous reactants, respectively; and S_o is the initial CaO surface area. Under the conditions of high solids concentration, A_{CaO} can be considered constant and equal to S_o in the initial stages of the reaction as the conversion is very low, and the initial rate can be rewritten as

$$-r_{init} = k'{P_{SeO_2}}^m \tag{5}$$

where k' is given by

$$k' = k{S_o}^n \tag{6}$$

Assuming that the reaction rate constant can be represented by Arrhenius equation, we can write

$$k' = A{S_o}^n \exp\left(\frac{-E_a}{RT}\right) \tag{7}$$

Substituting the expression for k' (eq 7) in the initial rate equation (eq 3), we get

$$-r_{init} = A{S_o}^n \exp\left(\frac{-E_a}{RT}\right){P_{SeO_2}}^m \tag{8}$$

At the initial stages of the reaction, the reaction rate can be represented as

$$-r_{init} = \left(\frac{x}{t}\right)\Big|_{t\to 0} \tag{9}$$

Therefore

$$\left(\frac{x}{t}\right)\Big|_{t\to 0} = A{S_o}^n \exp\left(\frac{-E_a}{RT}\right){P_{SeO_2}}^m \tag{10}$$

or

$$\left(\frac{x}{t}\right)\Big|_{t\to 0} = A' \exp\left(\frac{-E_a}{RT}\right){P_{SeO_2}}^m \tag{11}$$

where

$$A' = A{S_o}^n \tag{12}$$

For a constant P_{SeO_2}, the linear relationship between ln (x/t) and $(1/T)$ can be represented by

$$\ln\left(\frac{x}{t}\right)\Big|_{t\to 0} = \ln\left(A'{P_{SeO_2}}^m\right) - \left(\frac{E_a}{R}\right)\left(\frac{1}{T}\right) \tag{13}$$

From the slope of this linear curve, the activation energy value for the reaction can be determined.

For a constant reaction temperature (T), the linear relationship between ln (x/t) and ln (P_{SeO_2}) can be represented as

$$\ln\left(\frac{x}{t}\right)\Big|_{t\to 0} = -\left(\frac{E_a}{RT}\right) + \ln(A') + m \ln(P_{SeO_2}) \tag{14}$$

The slope of this curve represents the order of reaction for the reaction with respect to SeO_2 partial pressure, m.

The effect of initial sorbent surface area on the sorption of selenium oxide by CaO can be obtained from the linear relationship between $ln\ (x/t)$ and $ln\ (S_o)$ for constant temperature and SeO_2 partial pressure, as given below:

$$\ln\left(\frac{x}{t}\right)\Big|_{t\to 0} = B + n \ln(S_o) \tag{15}$$

TABLE 1. Chemical Composition and Structural Properties of CaO Powders Investigated

	in-house CaO (S1)	in-house CaO (S2)	CaO[a] (S3)
composition (wt %)			
CaO	97.0	97.0	98.5
SiO_2	0.9	0.9	0.3
Al_2O_3	0.6	0.6	0.3
MgO	1.0	1.0	0.9
Fe_2O_3	0.5	0.5	
mass median particle size, d_{50} (μm)	1.1	1.3	1.8
BET surface area (m^2/g)	52.0	35.0	3.0
pore volume (mL/g)	0.11	0.07	0.0

[a] Mississippi Lime Company, Ste. Genevieve, MO.

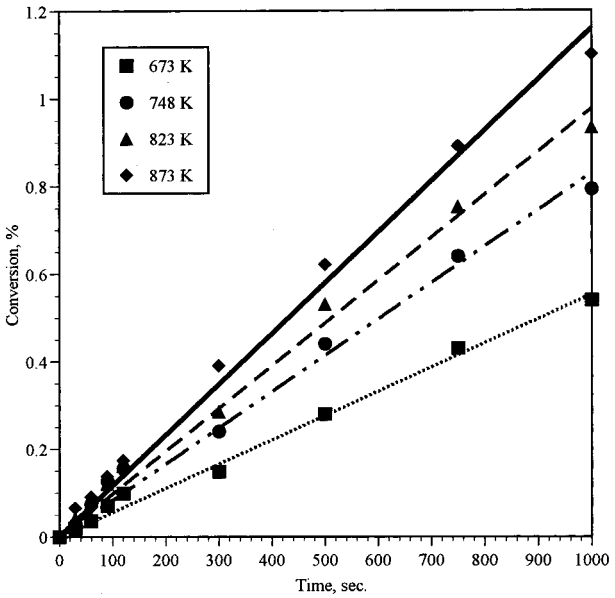

FIGURE 2. Effect of temperature on the reactivity of CaO. Initial CaO surface area, 3.0 m^2/g; P_{SeO_2}, 14.3 Pa.

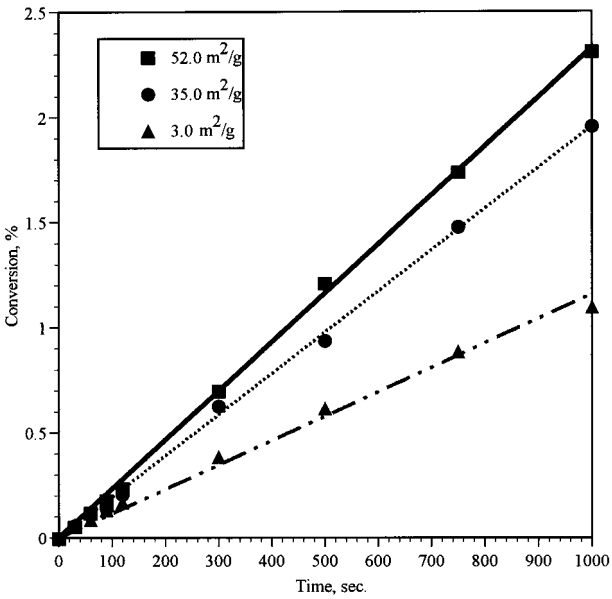

FIGURE 3. Effect of CaO initial specific surface area on CaO reactivity. Reaction temperature, 873 K; P_{SeO_2}, 6.6 Pa.

where B is a constant and is given by

$$B = \ln (A) + m \ln (P_{SeO_2}) - \left(\frac{E_a}{RT}\right) \qquad (16)$$

Results and Discussion

Kinetics of SeO_2−CaO Interaction. Sorption of SeO_2 with CaO is carried out under differential conditions in the temperature range of 400−600 °C. Duration of the reaction is varied from 30 to 1000 s. The partial pressure of SeO_2 in the gas phase is varied between 5 and 30 Pa, and three different types of CaO sorbents, each having different surface area and porosity, are investigated. Table 1 gives the chemical composition and initial structural properties of the sorbents investigated.

Reaction temperature, specific surface area, and the SeO_2 gas phase concentration are the principal parameters governing the rate of reaction between CaO and SeO_2 in the absence of pore diffusion limitations. The effects of these parameters on the reaction rate are shown in Figures 2−4. Smaller particle size (mass median particle diameter of <2.0 μm), small dispersed amount of particles, and the high gas velocities are used to eliminate all the external transport resistances. Emphasis is placed on gathering data for low conversion values (less than 5% solids conversion) in order to discount for structural changes and therefore intraparticle transport limitations due to the reaction.

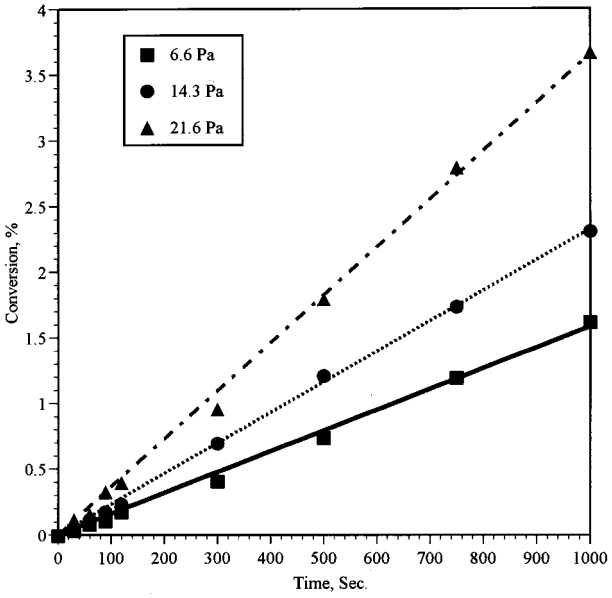

FIGURE 4. Effect of SeO_2 partial pressure on CaO reactivity. Initial CaO surface area, 52.0 m^2/g; temperature, 873 K.

The effect of reaction temperature on the sorption of selenium dioxide is shown in Figure 2, as obtained with CaO having a surface area of 3.0 m^2/g. The analysis of the postsorption solid sample shows the presence of $CaSeO_3$ as

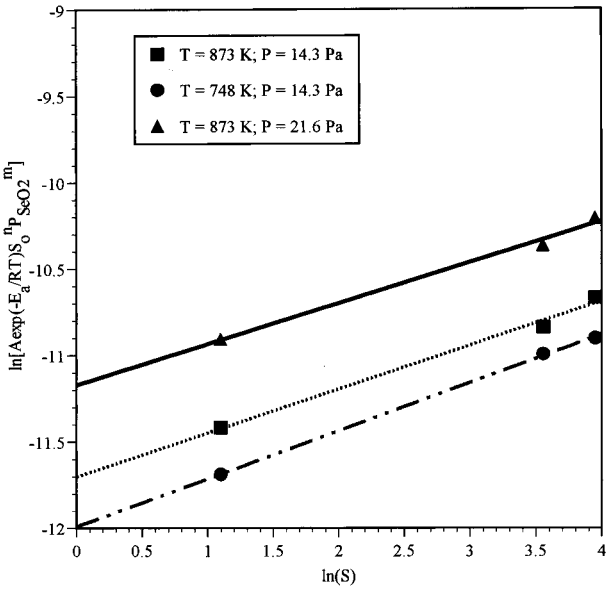

FIGURE 5. Determination of order of reaction with respect to CaO initial specific surface area at given reaction temperatures and SeO_2 partial pressures (average slope, $n = 0.25$).

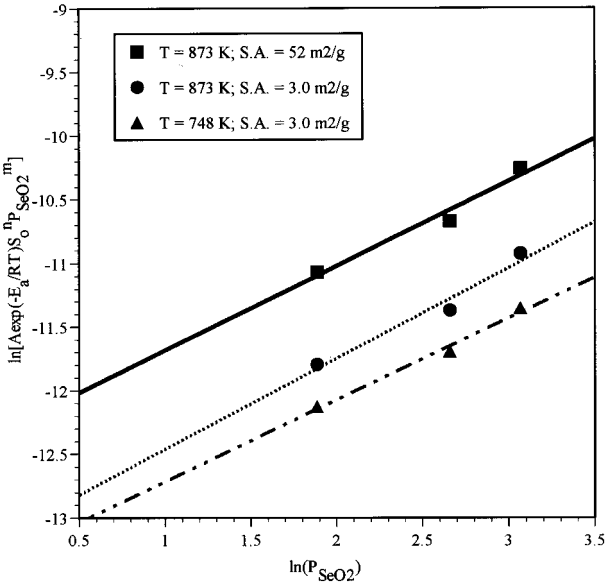

FIGURE 6. Estimation of reaction order m, with respect to SeO_2 partial pressure (average slope, $m = 0.66$).

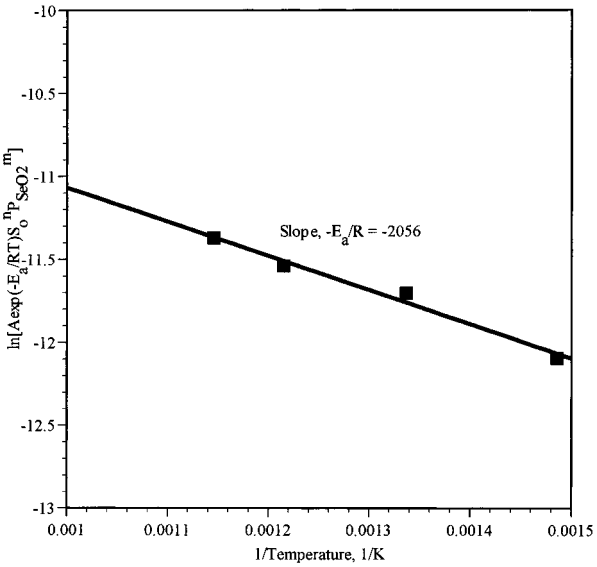

FIGURE 7. Estimation of activation energy of the reaction. Initial CaO surface area, 3.0 m^2/g; $P_{SeO_2} = 14.3$ Pa (activation energy, E_a, 4.03 kcal/gmol).

the sole product of this interaction. For a constant gas phase SeO_2 concentration (differential condition with respect to SeO_2) and initial sorbent surface area, the rate of the reaction (slope of the curve) should remain constant at a given temperature as observed from the Figure 2. It can be seen from these results that the effect of temperature is not very drastic. Similar behavior is also seen at various other values of SeO_2 partial pressure (5−30.0 Pa). These trends would suggest that the activation energy of the reaction is fairly low.

The effect of surface area on the reaction rate is obtained at a reaction temperature of 600 °C, and the results are shown in Figure 3. Measurement of sorbent conversion as a function of SeO_2 partial pressure is shown in Figure 4. Reaction rate increases with increasing SeO_2 partial pressure at a given temperature and the sorbent initial surface area.

The effect of surface area can be clearly determined by re-plotting the data shown in Figure 3. The rate of reaction (slope of the curve) is plotted logarithmically against the initial calcine BET surface area as shown in Figure 5 (eq 15). The average slope of the least-squares lines fitted to these data is 0.25, suggesting that the reaction rate varies with the surface area in a nonlinear manner.

The effect of gas phase SeO_2 concentration on extent of reaction is evaluated by logarithmically plotting the initial reaction rate as a function of SeO_2 partial pressure at a constant temperature and initial sorbent surface area (eq 14), as shown in Figure 6. The average slope of the line fitted to the data is about 0.66, the order of reaction with respect to the gas phase SeO_2 concentration, m in eq 3. Since the value of $m = 1$ would be expected for the diffusion of SeO_2 gas, the result could be interpreted as additional evidence of a rate process not involving gas diffusion and controlled by surface chemical reaction (*24*).

The slope of the curves obtained from the data of Figure 2 are plotted against temperature according to the Arrhenius relationship in Figure 7 (eq 13). The correlation observed is linear in the temperature range of this study, corroborating the assumption that pore diffusion resistance for less than 2.0 μm particles of low surface area (3.0 m^2/g) is negligible. The activation energy corresponding to the slope of the least-squares linear fit is 4.03 kcal/gmol (16.85 kJ/gmol). The observed activation energy is within the normal range of activation energies for slow reactions that exhibit low temperature dependence (*25*−*28*).

Simultaneous Sulfation and Selenition of CaO. The presence of SO_2 in the gas phase along with SeO_2 can result in various interactions. Possible interplay could involve a gas phase reaction between SO_2 and SeO_2; a gas−solid interaction between $CaSO_4$ and SeO_2, resulting in the formation of complexes such as $SeOSO_4$; or independent sorbent−species interaction with the formation of both $CaSO_4$ and $CaSeO_3$. To determine the effect of SO_2 on selenium capture, sorption experiments were carried out with 2.3 Pa partial pressure of SeO_2 in gas phase and SO_2 partial pressure varying from 100 to 400 Pa. Sorbent is exposed for a duration of 2 h in the presence of 16% O_2 and a total gas flow rate of 2.5 L/min. The presence of O_2 has no effect on SeO_2 capture by CaO as shown by Ghosh-Dastidar et al. (*19*). The results indicate that selenium capture is drastically reduced in the presence of SO_2. The possible reason for such a significant reduction is the preferential sulfation of the sorbent particles (due to high SO_2 concentration), which would lead to

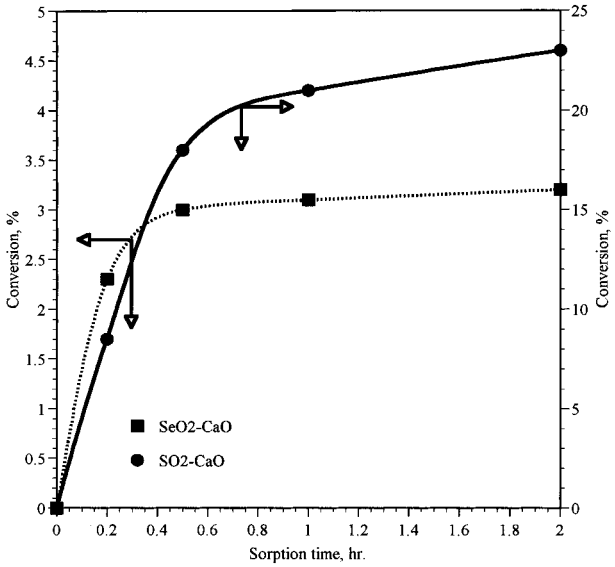

FIGURE 8. SeO_2 interaction with CaO in the presence of comparable concentration of SO_2. Sorption temperature, 873 K; P_{SO_2}, 30 Pa; P_{SeO_2}, 13 Pa.

extensive pore plugging/blocking due to the formation of a high molar volume $CaSO_4$ product, thus rendering the sorbent inaccessible for trace metal species. Assuming an initial CaO porosity of 35%, theoretical analysis suggests that 33% sorbent sulfation would reduce the overall porosity to 0% and would result in premature reaction termination for the sorbent particles.

To get a better understanding of simultaneous trace species and SO_2 capture by Ca-based sorbents, sorption experiments were designed such that the gas phase concentrations of SO_2 and SeO_2 were comparable. Sorbent particles are exposed to 13 Pa of SeO_2 and 30 Pa of SO_2 partial pressure, respectively, simultaneously, and the results of these experiments (presented in Figure 8) show a significant increase in the selenation of the sorbent, albeit the sulfation reaction still remains dominant.

Acknowledgments

This work was supported by Ohio Coal Development Office. The authors would like to acknowledge Mr. Huitang Jin and Mr. Shannon Lenze for their assistance with the analyses.

Glossary

A	preexponential factor in Arrhenius expression for reaction rate constant
A'	modified preexponential factor
A_{CaO}	available surface area of CaO
B	constant (eq 16)
E_a	activation energy of the reaction
k	specific reaction rate constant
k'	modified reaction rate constant
m	order of the reaction with respect to SeO_2 concentration
n	order of reaction with respect to initial sorbent-specific surface area
P_{SeO_2}	partial pressure of SeO_2 in the gas phase
r_{init}	initial reaction rate
R	universal gas constant
S_o	initial sorbent specific surface area
t	time
T	temperature
x	conversion of CaO

Literature Cited

(1) Cooper, W. C.; Benett, K. G.; Croxton, F. C. In *Selenium*; Zingaro, R. A., Cooper, W. C., Eds.; Van Nostrand Reinhold Co.: New York, 1974; pp 1−30.

(2) Wilbur, G. C. In *Selenium. A Potential Environmental Poison and a Necessary Food Constituent*; C. C Thomas Publisher: Springfield, IL, 1983.

(3) Fishbein, L. *Fundam. Appl. Toxicol.* **1983**, *3*, 411−419.

(4) Linak, W. P.; Wendt, J. O. L. *Prog. Energy Combust. Sci.* **1993**, *19*, 145−185.

(5) Martinez-Tarazona, R. M.; Spears, A. D. *Fuel Process. Technol.* **1996**, *47*, 79.

(6) Andren, A. W.; Klein, D. H.; Talmi, Y. *Environ. Sci. Technol.* **1975**, *9* (9), 856.

(7) Germani, M. S.; Zoeller, W. H. *Environ. Sci. Technol.* **1988**, *22* (9), 1079−1085.

(8) Allaway, W. H. *Trace Subst. Environ. Health* **1969**, *2*, 181.

(9) Marshall, E. *Science* **1986**, 231.

(10) Oehm, G. L.; Crisp, P. T.; Ellis, J. *J. Air Waste Manage. Assoc.* **1991**, *41*, 190.

(11) Sarquis, M.; Mickey, C. D. *J. Chem. Educ.* **1980**, *57*, 886.

(12) Valkovic, V. *Trace Elements in Coal;* CRC Press: Boca Raton, FL, 1983; Vol. 1.

(13) Davison, R. L.; Natusch, D. F. S.; Wallace, J. R.; Evans, C. A. *Environ. Sci. Technol.* **1974**, *8* (13), 1107−1113.

(14) Dismukes, E. B. *Fuel Process. Technol.* **1994**, *39*, 403−416.

(15) Uberoi, M.; Shadman, F. *AIChE J.* **1990**, *36* (2), 307−309.

(16) Uberoi, M.; Punkaj, W. A.; Shadman, F. *Prog. Energy Combust. Sci.* **1990**, *16*, 205.

(17) Uberoi, M.; Shadman, F. *Environ. Sci. Technol.* **1991**, *25* (7), 1285−1289.

(18) Gullett, B. K.; Raghunathan, K. *Energy Fuels* **1994**, *8*, 1068−1076.

(19) Ghosh-Dastidar, A.; Mahuli, S. K.; Agnihotri, R.; Fan L.-S. *Environ. Sci. Technol.* **1996**, *30*, 447−452.

(20) Ghosh-Dastidar, A.; Mahuli, S. K.; Agnihotri, R.; Fan L.-S. *Ind. Eng. Chem. Res.* **1996**, *35* (2), 598.

(21) Milne, C. R.; Silcox, G. D.; Pershing, D. W.; Kirchgessner, D. A. *Ind. Eng. Chem. Res.* **1990**, *29* (11), 2201.

(22) Mahuli, S. K.; Agnihotri, R.; Chauk, S.; Ghosh-Dastidar, A.; Fan L.-S. *Environ Sci Technol.* **1997**, *31*, 3226−3231.

(23) Selivonava, N. M.; Shneyder, V. A. *Khim. Khim. Tekhnol.* **1958**, *4*, 664−666.

(24) Borgwardt, R. H.; Bruce, K. R. *AIChE J.* **1986**, 32 (2), 239−246.

(25) Westmoreland, P. R.; Gibson, J. B.; Harrison, D. P. *Environ Sci. Technol.* **1971**, 11 (5), 488−491.

(26) Gokarn, A. N.; Doraiswamy, S. K. *Chem. Eng. Sci.* **1971**, *26*, 1521−1533.

(27) Sofekun, O. A.; Doraiswamy, L. K. *Ind. Eng. Chem Res.* **1996**, *35*, 3163−3170.

(28) Konttinen, J. T.; Zevenhoven, C. A. P.; Hupa, M. M. *Ind. Eng. Chem. Res.* **1997**, *36*, 2332−2339.

Received for review December 29, 1997. Revised manuscript received March 19, 1998. Accepted March 23, 1998.

ES971119J